https://doi.org/10.5194/egusphere-2025-1125
Preprint. Discussion started: 25 April 2025

Reviewer 1

Reviewer 2

The North Balearic Front as an ecological boundary: zooplankton fine-scale distribution patterns in late spring

Maxime Duranson[1,2], Léo Berline[1], Loïc Guilloux[1,3], Alice Della Penna[4,5], Mark D. Ohman[6], Sven Gastauer[2], Cédric Cotte[7], Daniela Bănaru[1], Théo Garcia[8], Maristella Berta[9], Andrea Doglioli[1], Gérald Gregori[1], Francesco D'Ovidio[7], and François Carlotti[1]

[1]Université Aix Marseille, Université de Toulon, CNRS, IRD, MIO, Marseille, France
[2]Thünen Institute of Sea Fisheries, Bremerhaven, Germany
[3]CNRS,Univ Brest, IRD, IFREMER, LEMAR, IUEM, F-29280 Plouzané,France
[4]Institute of Marine Science, University of Auckland, New Zealand
[5]School of Biological Sciences, University of Auckland, New Zealand
[6]Integrative Oceanography Division, Scripps Institution of Oceanography, La Jolla, California, USA
[7]Sorbonne Université, CNRS, IRD, MNHN, Laboratoire d'Océanographie et du Climat: Expérimentations et Approches Numériques (LOCEAN-IPSL), Paris, France.
[8]Aix Marseille University CNRS, Centrale Marseille, I2M, Marseille, France
[9]Istituto di Scienze Marine- Consiglio Nazionale delle Ricerche (ISMAR-CNR), Sede Secondaria di Lerici, 19032 La Spezia, Italy

Correspondence to: Maxime Duranson (maxime.duranson@thuenen.de), François Carlotti (francois.carlotti@mio.osupytheas.fr)

Keywords

BioSWOT-Med campaign, Northwestern Mediterranean Sea, Ocean Fronts, Vertical distributions, Copepod Community, Size, Trophic categories

Abstract

Observations, models and theory have suggested that ocean fronts are ecological hotspots, generally associated with higher diversity and biomass across many trophic levels. Nutrient injections are often associated with higher chlorophyll concentrations at fronts, but the response of the zooplankton community is still insufficiently understood. The present study investigates mesozooplankton stocks and composition during late spring, northeast of Menorca along two north-south transects that crossed the North Balearic Front (NBF) separating central water of the Northwestern Mediterranean Sea (NWMS) gyre from peripheral waters originating from the Algerian basin. During the BioSWOT-Med campaign, vertical triple-net tows were carried out at three depths (100, 200, and 400 m) with 200 µm and 500 µm meshes, and the samples were processed with ZooScan to classify organisms into eight taxonomic groups. Zooplankton distributions were analyzed for the surface layer (0–100 m), a mid-depth layer (100–200 m), and a deeper layer (200–400 m). The results showed no significant biomass increase at the front across all vertical layers. The NBF seems to act more like a boundary between communities rather than a pronounced area of active or passive zooplankton accumulation. Analysis of stratified vertical distributions of zooplankton highlighted distinct taxonomic compositions in the three layers, and a progressive homogenization of

https://doi.org/10.5194/egusphere-2025-1125
Preprint. Discussion started: 25 April 2025

community structure with depth, reflecting a weaker impact of hydrological processes on deeper communities. The front's clearest impact was within the upper 100 meters, where the taxonomic composition showed differences between the front and the adjacent water masses, with a decrease in all taxonomic groups except Cnidaria, which increased sharply. In the two deeper layers, the front also influenced community composition, although to a lesser extent, with marked increases in Foraminifera and Cnidaria. Moreover, the northern water mass and the front were dominated by large copepods, while the southern water mass exhibited higher zooplankton diversity and smaller-sized copepods. The results of this study highlight the complexity of processes shaping planktonic communities over time and space in the NBF zone and its adjacent waters. These processes include zooplankton stock reduction in the transitional post-bloom period, marked effect of diel variation linked to vertical migrations, and potentially the impact of storm-related mixing in the surface layer that can disrupt established ecological patterns.

1 Introduction

Oceanic fronts are narrow regions of elevated physical gradients that separate water parcels with distinct properties, such as temperature, salinity, and thus density (Hoskins (1982); Joyce (1983); Pollard and Regier (1992); Belkin and Helber (2015)). These frontal zones act as dynamic boundaries between distinct water masses (Ohman et al. (2012); Man´ko et al. (2022)), which play a crucial role in shaping marine ecosystems (Belkin et al. (2009)). Moreover, fronts display wide variations in spatial and temporal dimensions ranging from hundreds of meters to tens of kilometers, and from short-lived to permanent (Owen (1981); McWilliams (2016); Lévy et al. (2018)). Fronts are key structural features of the ocean, affecting all trophic levels across a wide range of spatial and temporal scales (Belkin et al. (2009)).

The relationships between fronts and plankton have received considerable attention in marine ecology due to the enhanced biological production and community changes that are sometimes observed in their vicinity (Le Fèvre (1987); Fernández et al. (1993); Pinca and Dallot (1995); Errhif et al. (1997); Pakhomov and Froneman (2000); Chiba et al. (2001); Munk et al. (2003)). As physical barriers or zones of mixing, fronts structure biomass and species distributions, generally leading to distinct ecological communities on either side (Ohman et al. (2012); Le Fèvre (1987); Prieur and Sournia (1994); Gastauer and Ohman (2024)). Fronts are often associated with high phytoplankton abundance, supporting elevated zooplankton stocks and metabolism (Thibault et al. (1994); Ashjian et al. (2001); Ohman et al. (2012); Derisio et al. (2014); Powell and Ohman (2015a)). Frontal structures can enhance primary and secondary production essentially by promoting nutrient input through cross-frontal mixing and vertical circulation driven by horizontal density gradients (Durski and Allen (2005); Liu et al. (2003); Derisio et al. (2014); Russell et al. (1999). These nutrient-rich conditions (bottom-up) sometimes fuel elevated chlorophyll concentrations, supporting the aggregation of zooplankton, fish larvae, and their predators such as tuna, sharks, seabirds and whales (Herron et al., 1989Herron et al. (1989); Olson et al. (1994); Royer et al. (2004); Queiroz et al. (2012); di Sciara et al. (2016); Druon et al. (2019)). Pronounced changes in zooplankton diel vertical migration (DVM) behaviour have also been observed across frontal gradients (Powell and Ohman (2015b), Gastauer and Ohman (2024)).

https://doi.org/10.5194/egusphere-2025-1125
Preprint. Discussion started: 25 April 2025

Recent studies (Mangolte et al. (2023); Panaïotis et al. (2024)) have highlighted the importance of investigating zooplankton distribution at fine scales and their patchiness in the vicinity of fronts to understand their interactions with particles (e.g., organic detritus and prey items) and the environment. Mangolte et al. (2023) revealed that the plankton community exhibits fine-scale variability across fronts, with biomass peaks of different taxa often occurring on opposite sides of the front, or with different spatial extents. This fine-scale cross-frontal patchiness suggests processes that spatially segregate plankton taxa, leading to the formation of multiple adjacent communities rather than a single coherent frontal plankton community.

The BioSWOT-Med cruise offered a unique opportunity to investigate how mesoscale oceanographic features influence zooplankton communities across the NBF, which separates the water masses of the Provencal Basin to the north and the Algerian Basin to the south. In the NWMS, the role of mesoscale structures in the open ocean such as density fronts and eddies on the distribution and diversity of zooplankton has already been widely documented (Saiz et al. (2014)). These structures generally increase the patchiness and activity of plankton, and stimulate trophic transfers to large predators (Cotté et al. (2009), Cotté et al. (2011)). However, among the most pronounced geostrophic frontal zones in the NWMS, the NBF and its ecological impacts are the least studied.

This interdisciplinary campaign combined satellite observations with a wide range of in situ measurements, including current profiling, vertical velocity, radiation, moving vessel profilers, gliders, drifters, floats, biogeochemical analyses, genomics, phytoplankton and zooplankton sampling, and megafauna observations. Zooplankton communities were sampled using various net tows, providing insights into their composition and spatial variability across frontal gradients. In this study, we hypothesize that the structure of zooplankton communities differs between the water masses on either side of the front, reflecting both the barrier effect of the front and the distinct origins of the two water masses. This hypothesis raised several questions, which we aimed to address in this study: how are zooplankton communities structured on each side of the front; is the zooplankton community at the front a mixture of communities from both sides, or does it form a distinct community; does the front influence the vertical structure of zooplankton communities; and can weather events, such as storms, influence the structure of zooplankton communities within the water masses?

2 Materials and methods

2.1 Study area

The study was conducted in the NWMS (Fig. 1) as part of the BioSWOT-Med cruise, and specifically in the frontal zone associated with the Balearic current. Due to its coastal proximity, the frontal zones of the Northern Current (NC) (Fig. 1) have been widely studied from physical and ecosystem perspectives, on both the Ligurian (Prieur et al. (1983); Stemmann et al. (2008)) and Catalan sides (Font et al. (1988); Sabatés et al. (2007)). Downstream of the NC, the North Balearic current flows from northeast Menorca to southwest Corsica. This current is associated with the NBF, which marks the transition between two contrasting surface water masses: the saltier, colder, and more productive waters from the Provençal Basin to the north (hereafter referred to as water mass **A**), and the fresher, warmer, and less productive waters

https://doi.org/10.5194/egusphere-2025-1125
Preprint. Discussion started: 25 April 2025

from the Algerian Basin to the south (hereafter referred to as water mass **B**). The sharp frontal region separating them is designated as **F** (Fig. 2). Recent contributions from glider data and satellite imagery have enabled us to better characterize the NBF (Barral (2022)). Its latitudinal position varies seasonally (from 40.2° N in spring to 41° N in autumn) and interannually. These shifts are linked to the intensity and extent of winter deep convection in the northern Provençal Basin, and to mesoscale dynamics to the south, where lighter Atlantic waters are advected northward between Menorca and Sardinia (Millot (1999); Seyfried et al., 2019)).

The BioSWOT-Med cruise (https://doi.org/10.13155/100060; PIs: A. Doglioli and G. Grégori) was performed on board the R/V L'Atalante (FOF-French Oceanographic Fleet) from 21 April to 14 May 2023 in an area about 100 km north-east of Menorca Island (NWMS) (Fig. 2). Figure 2.a shows the zone as observed four days before the first transect, due to cloud cover during the first days of the survey (Fig. A1).

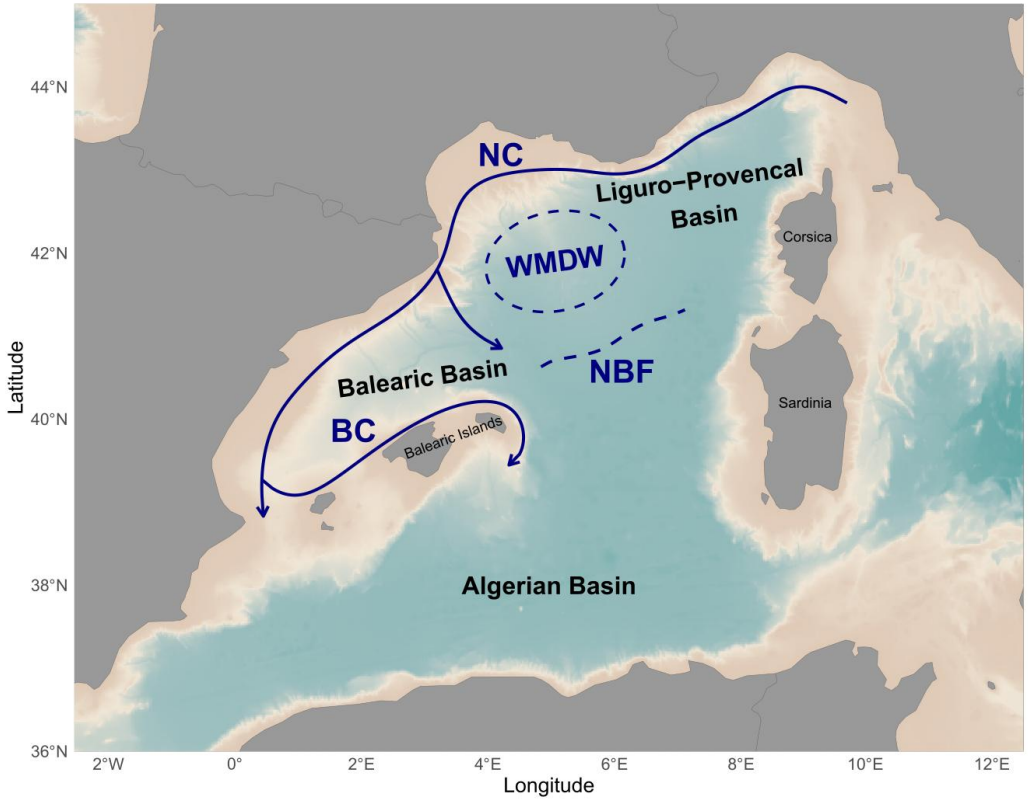

Figure 1. Maps of the NWMS showing the major oceanographical currents and front (NC: Northern Current, BC: Balearic Current, NBF: North Balearic Front, WMDW: Western Mediterranean Deep Water formation area) of the northern part of the NWMS. After Millot (1987), López García (1994) and Pinardi and Masetti (2000).

https://doi.org/10.5194/egusphere-2025-1125
Preprint. Discussion started: 25 April 2025

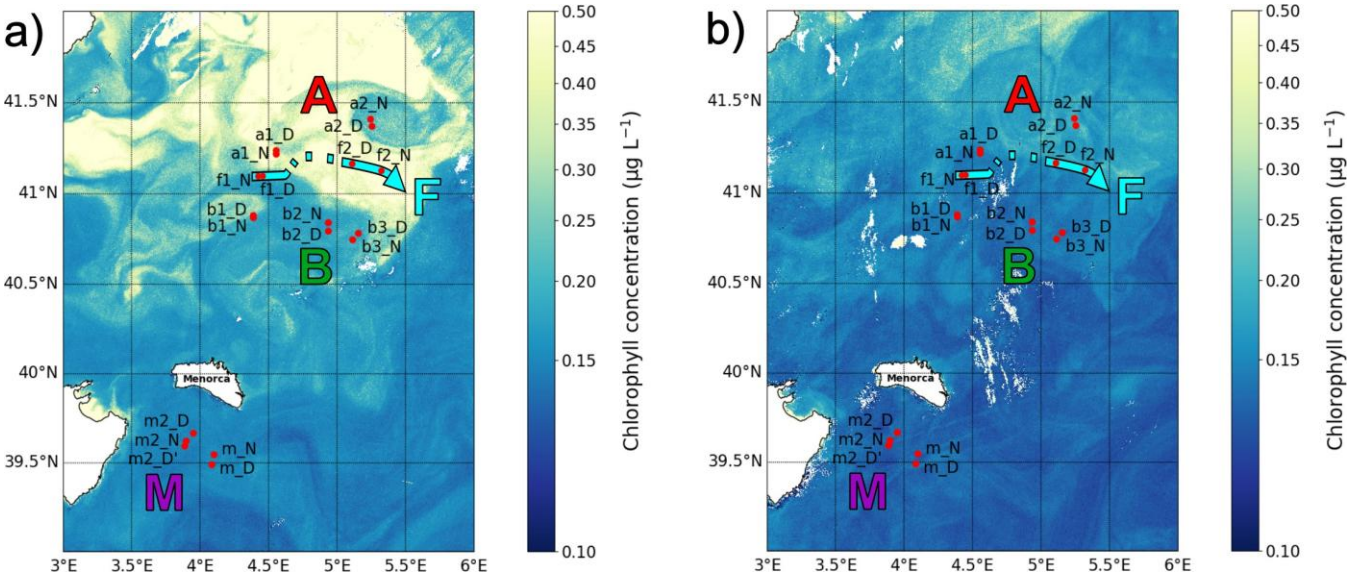

Figure 2. Maps of the sampling stations with surface chlorophyll concentration (μg L-1) from Sentinel 3. a) Map from April 21 showing conditions 4 days before the first transect. b) Map from May 5 showing conditions during the second transect. The colors representing the three water masses and the front will be maintained throughout the paper.

2.2 Sample strategy

The strategy of the cruise was designed to take advantage of the novel SWOT (Surface Water and Ocean Topography) satellite mission, in order to better resolve fine-scale oceanic features. During the "fast sampling phase," SWOT provided altimetry data characterized by high spatial resolution (2 km) and a 1-day revisit period over 150 km-wide oceanic regions. With the support of the international SWOT AdAC (Adopt-A-Crossover, https://www.swot-adac.org/; PI F.d'Ovidio) Consortium, the BioSWOT cruise applied an adaptive multidisciplinary approach by combining daily SWOT images and environmental bulletins provided by the SPASSO toolbox (https://spasso.mio.osupytheas.fr/, Rousselet et al., (2025)). Along with in situ measurements taken using a suite of instruments to capture physical, chemical and biological properties (Doglioli et al. (2024), cruise report). This strategy enabled the targeting of fine-scale features (e.g., kilometers) of the NBF.

The three main water masses (A, B, F) were each sampled at two stations: a1 and a2, b1 and b2, f1 and f2; with a1, b1, f1 on the first transect (westbound) and a2, b2, f2 on the second transect (eastbound). Each station was sampled twice: at day (noon) and night (midnight). Additionally, three supplementary stations (b3, m, and m2) were sampled (Table 1, Fig. 2). At each station, the vessel remained within the same water mass for 24 hours, drifting slightly with the currents during the sampling period, which explains the small differences in station location between day and night (Fig. 2). The two f2 stations were relatively distant from each other due to a strong frontal current.

Because of a storm (2nd May), a third area, "M", was sampled twice while the ship took shelter south of Menorca and conducted similar measurements as in zones A, B, and F. The M zone is different from the three other sampled zones in terms of bathymetry (Table 1), as it was located around 20 km from the continental shelf. On the way home, a final station was sampled in B (Table 1). At every station, physical properties were recorded using a CTD rosette, which was deployed four times daily at fixed intervals (06:00, 12:00, 18:00, and 00:00 local time). Hereafter, water masses will be designated by an uppercase letter (A, B, M, and F for the front), and stations by a lowercase letter (*a*, *b*, *m*, *f*).

https://doi.org/10.5194/egusphere-2025-1125
Preprint. Discussion started: 25 April 2025

Table 1. Station details. In Station Name, 'D' stands for Day and 'N' stands for Night. Depth values are approximate (±50 m) for the station within the water mass M. Depths indicated as ">2500" correspond to stations deeper than 2500 m.

Campaign Stage	Station Name	Water Mass	Date - Time	Latitude	Longitude	Depth (m)
1st transect	a1_D	A	25/04 - 12:38	41.240	4.553	>2500
	a1_N	A	26/04 - 00:02	41.224	4.563	>2500
	f1_D	Front	26/04 - 12:11	41.099	4.423	>2500
	f1_N	Front	27/04 - 00:32	41.102	4.456	>2500
	b1_N	B	28/04 - 00:17	40.874	4.388	>2500
	b1_D	B	28/04 - 12:28	40.884	4.389	>2500
Storm	m_N	M	02/05 - 00:37	39.555	4.101	1350
	m_D	M	02/05 - 12:22	39.493	4.087	1500
2nd transect	b2_D	B	04/05 - 12:16	40.795	4.933	>2500
	b2_N	B	05/05 - 00:13	40.849	4.936	>2500
	f2_D	Front	05/05 - 11:49	41.175	5.108	>2500
	f2_N	Front	06/05 - 00:45	41.134	5.308	>2500
	a2_N	A	07/05 - 00:13	41.412	5.24	>2500
	a2_D	A	07/05 - 12:15	41.376	5.253	>2500
Return water mass M	m2_D	M	10/05 - 11:31	39.671	3.957	1150
	m2_N	M	11/05 - 00:31	39.629	3.902	1200
	m2_D'	M	11/05 - 11:53	39.603	3.885	1300
Return water mass B	b3_D	B	12/05 - 12:15	40.782	5.152	>2500
	b3_N	B	12/05 - 23:58	40.746	5.112	>2500

2.3 Zooplankton collection

Zooplankton samples were collected using a triple net (Triple-WP2) equipped with three individual nets, each with a 60 cm mouth diameter but different mesh sizes (500 μm, 200 μm, 64 μm). For this study, which focuses on mesozooplankton, only the samples collected by 200 and 500 μm nets were used. The nets were deployed vertically to cover three integrated layers (400-0 m, 200-0 m, 100-0 m). Note that the net deployed to 400 m at station *m_N* could not be analyzed because it was found folded up on itself upon retrieval. The filtered water volume was not measured with a flowmeter but estimated from the net mouth area and the towing distance. After collection, samples were preserved in 4% borate-buffered formaldehyde.

https://doi.org/10.5194/egusphere-2025-1125
Preprint. Discussion started: 25 April 2025

2.4 Zooplankton sample processing

In a shore-based laboratory (Mediterranean Institute of Oceanography (MIO), Marseille, France), samples were digitized with the ZooScan digital imaging system (Gorsky et al. (2010)) to identify and determine the size structure of the zooplankton communities. Each sample, from the 200 and 500 μm nets, was divided into one of two size fractions (<1000 and >1000 μm) for better representation of rare large organisms in the scanned subsample (Vandromme et al. (2012)). Each fraction was split using a Motoda box (Motoda (1959)) until it contained an appropriate number of objects, approximately 1500, according to Gorsky et al. (2010). After scanning, each image was processed using ZooProcess (Gorsky et al. (2010)), which is written in the ImageJ image analysis software (Rasband, 1997–2011). Only objects having an Equivalent Circular Diameter (ECD) > 300 µm were detected and processed (Gorsky et al., 2010). Objects were automatically classified using EcoTaxa (https://ecotaxa.obs-vlfr.fr/) on Zooscan images with a pixel size of 10.58 µm. Consequently, some taxa could be identified to the species level, while others could only be resolved to genus, family, or order. Certain taxa were either too small or could not be precisely recognized by EcoTaxa for other reasons (e.g., sample quality, image quality during scanning) and therefore could not be assigned to a taxonomic level finer than the order. For example, 65% of copepods were classified as *Calanoida undetermined*. Consequently, although 101 taxa were detected, they have been grouped into eight main categories: Appendicularia, Chaetognatha, Copepoda, Cnidaria, Eumalacostraca, Foraminifera, Thaliacea, and Other_Organisms (Table 2). Table 2 does not list all recognized taxa within each of the eight categories, but only those that accounted for at least 1% of the total concentration within their category. The last category, Other_Organisms, includes all remaining taxa that did not belong to any of the designated classes and were present in very low numbers across all samples. Zooplankton concentration (number of individuals m−3) was calculated from the number of validated vignettes in ZooScan samples, considering the scanned fraction and the sampled volume from the nets.

The 200 and 500 µm net samples were processed separately using ZooScan, and their resulting counts were subsequently combined. To avoid double counting of organisms large enough to be captured by both nets, a threshold value was established, based on the analysis of the Normalized Biomass Size Spectra (NBSS) (Sect. 2.8), considering all stations and depths (a specific value for each station would not have significantly altered the results). The threshold value (1148 μm ECD) identified the body size at which the 500 μm net samples more effectively (Fig. A2). Thus, organisms smaller than this size from the 200 μm net, and those larger from the 500 μm net, were combined to form a new count, called 'combined net' hereinafter.

Table 2. Zooplankton taxonomic categories and their representative groups (≥ 1% of the concentration within their category) identified by ZooScan.

Category	Abbreviation	Representative Taxonomic Group identified by ZooScan
Appendicularians	App	Oikopleuridae, Fritillariidae, Appendicularia undetermined
Chaetognatha	Cha	Chaetognatha undetermined
Cnidaria	Cni	Cnidaria (ephyra), Hydrozoa, Siphonophorae, Physonectae, Trachylinae (*Aglaura*, *Solmundella*), Diphyidae
Copepoda	Cop	Calanoida undetermined, *Oithona*, *Centropages* (*Centropages typicus*, *Centropages* undetermined), Oncaeidae, *Pleuromamma* (*Pleuromamma* undetermined, *Pleuromamma abdominalis*), Corycaeidae (Corycaeidae undetermined, *Urocorycaeus*), *Euchaeta*
Eumalacostraca	Eum	Euphausiacea larvae, Amphipoda (*Phronima*, Amphipoda undetermined, Hyperiidae undetermined), Eumalacostraca undetermined, Decapoda (Dendrobranchiata), Euphausiacea undetermined
Foraminifera	For	Foraminifera undetermined
Thaliacea	Tha	Doliolida, Thaliacea undetermined, Salpida (Salpida undetermined, *Salpa fusiformis*)
Other Organisms	Oth	Limacinidae, Ostracoda, Errantia, Pteropoda (Pteropoda undetermined, Cymbuliidae), Crustacea (Crustacea undetermined, nauplii)

https://doi.org/10.5194/egusphere-2025-1125
Preprint. Discussion started: 25 April 2025

2.5 Definition of reconstructed depth layers: 100-200 m and 200-400 m

Our nets sampled the layers: 0-100, 0-200, and 0-400 meters (Sect. 2.3). In order to study the community as a function of depth, the concentration of different taxonomic groups (Sect. 2.4) was calculated in each layer by differencing. For instance, subtracting the concentration measured at 0-100 m from that at 0-200 m provided values for the 100-200 m layer. A similar approach was used to determine the values for the 200-400 m layer. This approach was assumed valid as the net tows were carried out successively within a relatively short interval of time, typically 45 minutes, although potential limitations are discussed in Section 4.4. It is important to note that subtractions were performed on the eight major categories and not on each taxonomic group (see Table 2). In rare cases (12%), especially for Eumalacostraca (particularly in the 100-200 m layer) and Cnidaria (particularly in the 200-400 m layer), resulting concentrations were negative and thus set to zero.

2.6 Analysis of variance

Using R version 4.4.1 (Team (2025)), one-way analyses of variance (ANOVA) were conducted to examine differences in absolute concentration across each taxonomic category. Prior to performing the ANOVA, the normality of residuals was assessed using the Shapiro-Wilk test and the homogeneity of variances verified with Levene's test (car package, version 3.1-3; Fox and Weisberg (2019)). ANOVAs were then performed for five factors: Water masses, Layer, Period (day or night), Transects (storm effect) and Copepod subgroups (DVM patterns). Copepod subgroups were selected based on a threshold of total concentration greater than 1% of the overall copepod assemblage, which resulted in the selection of seven taxa. For each significant ANOVA result ($p < 0.05$), a Tukey's Honest Significant Difference test was applied to identify the groups that differ substantially from one another.
In addition, a permutational multivariate analysis of variance (PERMANOVA) was used to test for differences in community composition among water masses. The analysis was performed on Hellinger-transformed relative concentrations of taxonomic groups, with significance assessed using 999 permutations.

2.7 Normalized Biomass Size Spectra (NBSS)

The size of organisms is considered a key indicator of community dynamics (Platt and Denman (1977)). NBSS (Platt and Denman (1977)) are widely used to study this property. For constructing the NBSS, zooplankton organisms were grouped into logarithmically increasing size classes. The total biovolume of each class was then divided by the width of its size class (Platt and Denman (1977)). The x-axis [log2 zooplankton biovolume ($mm^3.ind^{-1}$)] was calculated as:

$$\log_2 \frac{\text{Zooplankton biovolume } (mm^3.m^{-3})}{\text{Concentration of each class size } (ind.m^{-3})} \quad (2)$$

The y-axis [log2 normalized biovolume (m^{-3})] was calculated as:

$$\log_2 \frac{\text{Zooplankton biovolume } (mm^3.m^{-3})}{\text{Interval of each class size } (\Delta\text{volume } (mm^3))} \quad (3)$$

https://doi.org/10.5194/egusphere-2025-1125
Preprint. Discussion started: 25 April 2025

The NBSS thus represents the normalized biovolume as a function of the size of the organisms, both on a logarithmic scale. Biovolume data were estimated from ECD data provided by ZooProcess, using spherical approximation, which ensures a consistent metric for combining the two mesh sizes (200 and 500 µm).

To investigate community characteristics across water masses and the front, a taxonomic and size-based analyses were conducted focusing on copepods, which were the most abundantly sampled group. PCA_Size (Sect. 2.9) was applied to copepod concentrations per size at the different stations, using the size classes defined for the NBSS (Fig. A2). For clarity, the 15 original size classes were grouped into five, and each class was defined by its ECD rather than biovolume. Other taxonomic groups were not included because their larger size ranges and the rarity of large individuals, including organisms such as chaetognaths or cnidarians, introduced significant noise into the NBSS.

2.8 Principal Component Analysis (PCA)

PCA was used to evaluate the similarities between the stations based on the concentration of the different taxonomic groups. Distances between these stations were measured in the PCA phase space after Hellinger transformation, which allows us to use relative concentrations rather than absolute concentrations. Using absolute concentrations would mainly discriminate between the first and second transects and would not reveal a stable gradient between water masses. Legendre and Gallagher (2001) also showed that the Hellinger transformation, prior to PCA, is often preferable to Euclidean distance for calculating distances between samples. Hellinger distance (Rao (1995)) is obtained from:

$$D(x_1, x_2) = \sqrt{\sum_{j=1}^{p} \left(\sqrt{\frac{y_{1j}}{y_{1+}}} - \sqrt{\frac{y_{2j}}{y_{2+}}} \right)^2}, \quad (4)$$

where p denotes the number of categories, y_{ij} is the concentration of category j at station i, and y_{i+} is the sum of the concentrations of the ith object.

With this equation, the most abundant species contribute significantly to the sum of squares. The advantage of this approach is that it is asymmetric, meaning that shared absences (double zeros) do not increase similarity, unlike Euclidean distance, where they do (Prentice (1980); Legendre and Legendre (2012)).

The Hellinger transformation was performed with the labdsv package (Roberts (2023)). The concentration tables were centered and scaled, and the PCA was computed using FactoMineR (Lê et al. (2008)). Prior, to carrying out PCAs, the Hellinger-transformed data were checked for normality using the Shapiro-Wilk test. Correlations between taxonomic groups were assessed with Bartlett's test of sphericity to ensure sufficient linear structure for PCA.

Stations M were not included in the main PCAs, as their inclusion can obscure the frontal signal. However, their positions as supplementary individuals are shown in the PCA plots provided in the Appendix.

https://doi.org/10.5194/egusphere-2025-1125
Preprint. Discussion started: 25 April 2025

2.8.1 Fixed PCA axis for comparison across layers

To obtain comparable results across depth layers, the PCAs were always conducted in the same way with fixed axes. First, a PCA is performed using data from the 0–400 m layer. Then the datasets from all three layers were projected onto the 0-400 m layer's pair of PCA axes. This approach ensured that comparisons between communities in the three different layers were valid.

2.1.1 Pseudo-F calculation

To quantify the separation of each water mass (A, B, F) in PCA space, the pseudo-F (Calin´ski and Harabasz (1974)) was used. Dispersion was calculated as the sum of squared Euclidean distances of individuals to their group centroid (intra-group dispersion), while inter-group dispersion was defined as the sum of squared distances between group centroids and the global centroid, weighted by group size. The pseudo-F statistic is then:

$$\text{Pseudo-F} = \frac{\text{Inter-group dispersion}/(k-1)}{\text{Intra-group dispersion}/(n-k)}, \quad (5)$$

where k is the number of groups and n the total number of individuals.

A high pseudo-F value suggests a clear separation between groups, indicating that inter-group variation predominates over intra-group variation.

2.1.2 PCA with theoretical *f* stations

A fundamental question was whether the zooplankton community at the front represents a mixture of those from water masses A and B, or a distinct community. To address this, we created theoretical f{t} stations, defined as linear combinations of the communities observed at stations a and b, as close as possible (i.e., minimal distance) to the observed *f* stations. The combination of *a* and *b* follows the formula:

$$f\{t\} = \alpha \cdot a + (1-\alpha) \cdot b, \quad (6)$$

where α is the proportional contribution from stations *a* and *b*. A total of 101 iterations was performed, with α varying from 0 to 1 in increments of 0.01, generating four new theoretical stations per iterations:

$$f1\{t\}\_D = \alpha_1 \cdot a1\_D + (1-\alpha_1) \cdot b1\_D$$
$$f1\{t\}\_N = \alpha_1 \cdot a1\_N + (1-\alpha_1) \cdot b1\_N$$
$$f2\{t\}\_D = \alpha_2 \cdot a2\_D + (1-\alpha_2) \cdot b2\_D$$
$$f2\{t\}\_N = \alpha_2 \cdot a2\_N + (1-\alpha_2) \cdot b2\_N$$

https://doi.org/10.5194/egusphere-2025-1125
Preprint. Discussion started: 25 April 2025

These *f{t}* stations were then projected as supplementary points onto the PCA computed from the original *a*, *b*, and *f* stations; thus, they did not influence the axes or the positions of observed stations. For each iteration, the coordinates of the *f{t}* stations in the PCA space were obtained, and their distances to the corresponding observed f stations were calculated. The total distance (sum of all *f–f{t}* distances) was then computed for each transect. Finally, the *f{t}* station with the minimum total distance, along with its α value, was selected. This procedure generated intermediate observations that best reflect the theoretical composition of the front as a linear combination of *a* and *b*.

3 Results

3.1 Total concentration across water masses and layers

The absolute values of concentration of zooplanktonic organisms across different depth layers and stations (Fig. 3) revealed distinct temporal and spatial patterns. In general, concentrations in stations within the same water mass decreased over time (stations are presented in chronological order in Figure 3), with the exception for the front.

Regarding the spatial differences during the two front crossings, concentration is lower at the front, than in water masses A and B for the first transect. Indeed, values at the front were 2.9 times lower compared to water mass A and 1.4 times lower compared to water mass B. Interestingly, the second transect reveals greater homogeneity among water masses with values at the front only 1.1 times higher compared to water mass A and 1.9 times higher compared to water mass B, reflecting the potential influence of post-storm dynamics.

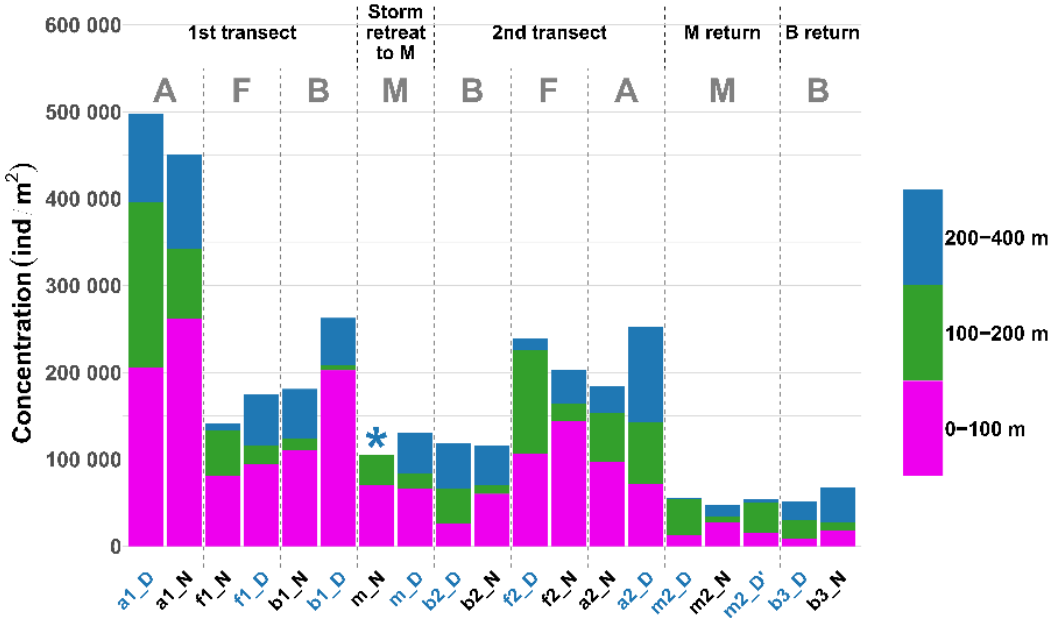

Figure 3. Stacked bar plot showing the concentration of zooplankton by intermediate layers and across all sampled stations. Stations are in chronological order. The asterisk (*) indicates that the 200–400 m net at station *m_N* could not be analyzed. Colors of stations names refers to the period of the day (blue for midday and black for midnight).

https://doi.org/10.5194/egusphere-2025-1125
Preprint. Discussion started: 25 April 2025

3.2 Taxonomic composition across nets and depth layers

The 200 μm net more efficiently captures copepods, which constitute 45–95% of the relative concentrations of taxa in the 0-200 m layer, while copepod concentrations comprise only 5-55% in the 500 μm net (Fig. 4). The larger mesh size is particularly effective for sampling larger taxa such as Appendicularia, Thaliacea, Eumalacostraca, Foraminifera, Cnidaria and Chaetognatha. The combined samples, which include contributions from both mesh sizes, still heavily reflect the taxa distributions observed in the 200 μm net, the concentrations of larger organisms sampled with the 500 μm net being low. This pattern was also observed in the layers 0-100 m and 0-400 m. Moreover, during the second transect (after the storm) the dominance of copepods is enhanced in water masses A and F.

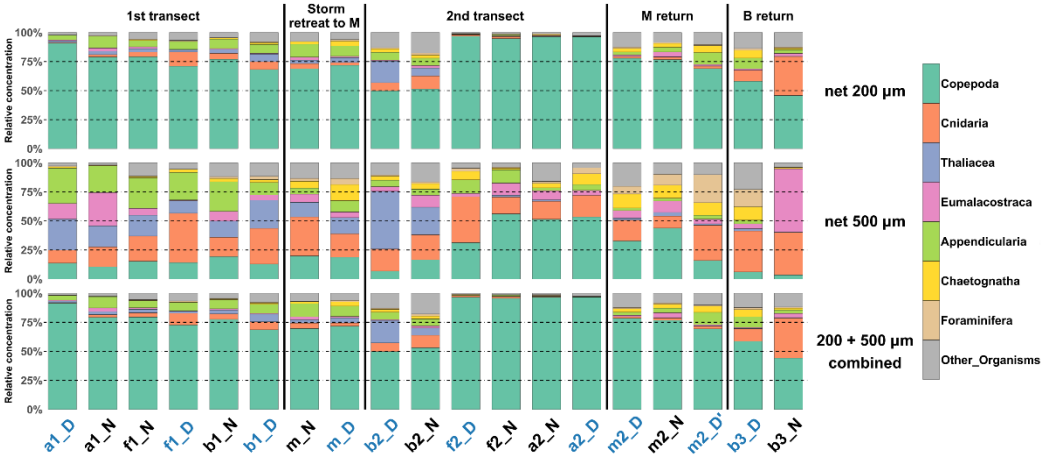

Figure 4. Relative concentration of taxonomic groups for nets deployed from the surface to a depth of 200 m, for the two mesh sizes (200 μm top, and 500 μm, middle) across all sampled stations (chronological order). Bottom: Relative concentration combining the two mesh sizes. Colors of stations names refers to the period of the day (blue for midday and black for midnight).

In the 0–100 m layer, copepods consistently dominate (Fig. 5), comprising at least 45% of the total concentration at nearly all stations (except for *b2_N*). In the 100–200 m layer there is marked heterogeneity with many stations (8 out of 18) showing less than 60% copepods. The 200–400 m layer returns to a dominance of copepods at most stations (15 out of 18), with the notable exceptions of station *b2_N*, where Eumalacostraca account for an anomalously high 55% of the sampled taxa, and *b3_N* where Cnidaria account for an anomalously high 67% of the sampled taxa.

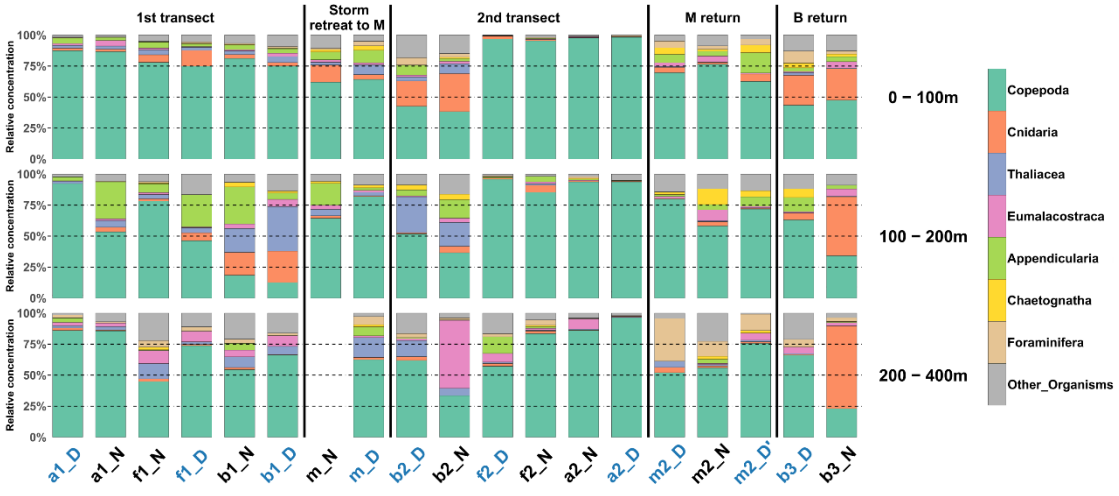

Figure 5. Relative concentration of taxonomic groups for the combined nets for the three intermediate layers across all sampled stations (chronological order). The net from station *m_N* at a depth of 400 m could not be analyzed. Colors of stations names refers to the period of the day (blue for midday and black for midnight).

https://doi.org/10.5194/egusphere-2025-1125
Preprint. Discussion started: 25 April 2025

3.3 Diel variations in vertical structuring of zooplankton stocks

Zooplankton communities seemed to show a vertical pattern. With the upper (0–100 m) and deeper (200–400 m) layers more similar to each other, and the mid-depth layer (100–200 m) more distinct. (Fig. 5). Hellinger distance analysis for the eight taxonomic groups reflected this pattern: the lowest distances were observed between the 0–100 m and 200–400 m layers for Copepoda (0.04 and 0.09 for the first and second transect, respectively), Eumalacostraca (0.03 and 0.08), and Other_organisms (0.06 and 0.03), whereas distances involving the 100–200 m layer were approximately four times higher.

A DVM pattern was evident in the two migrant groups, Copepoda and Eumalacostraca. At night, the 0–100 m and 100–200 m layers were more similar, while during the day, similarity was greater between the 100–200 m and 200–400 m layers. These patterns were statistically significant (post-hoc, $p < 0.001$ and 0.008, respectively). Hellinger distances between the surface (0–100 m) and deep (200–400 m) layers increased during both day (0.24 and 0.13 for Copepoda; 0.48 and 0.38 for Eumalacostraca) and night (0.29 and 0.34 for Copepoda; 0.38 and 0.52 for Eumalacostraca). In contrast, night-time distances between 0–100 m and 100–200 m were 8 times lower for Copepoda and 3 times lower for Eumalacostraca, while day-time distances between 100–200 m and 200–400 m were 21 and 5 times lower, respectively.

3.4 Community structure and water mass differentiation

3.4.1 Community composition across depths and water masses

PCA_Community summarizes the taxonomic composition of zooplankton communities across water masses and depths (Fig. 6). PCA_Community with stations M included as supplementary individuals is provided in Appendix (Fig. A4). Axis 1 is inversely correlated to copepod concentration, which stems from the extreme dominance of this group. Axis 2 appears to be more to characteristics of other groups ranging from pure filter feeders (Appendicularians and Thaliacea) to carnivores (Chaetognatha and Cnidaria), and to omnivores (Eumalacostraca, Other_organisms), Formanifera being at the extreme.

Copepods are more abundant in water masses A and the front, while other groups, notably Foraminifera, Cnidaria, Eumalacostraca, and Other_Organisms, dominate in water mass B. This results in a consistent proximity between the zooplankton communities of water mass A and the front across all layers, particularly pronounced during the second transect.

3.4.2 Comparison of the front community composition with adjacent waters

The relative concentrations of taxonomic groups across all stations, sorted by water mass and averaged across the three sampled layers, are used to compare the community compositions (Fig. 7). Results clearly reveal that the front appears very similar to water mass A in terms of the relative concentration of copepods which progressively decreases from A to F to B. To further investigate these observations, a PERMANOVA was conducted on the concentration of the entire community. No significant difference was found between A and F ($p = 0.312$). However, significant differences were observed between B and F ($p = 0.038$) and between A and B ($p = 0.006$). For copepods, significant differences were found between all pairs of water masses and for both transects, as determined by an ANOVA, except between F and A ($p = 0.406$ for the first transect and p =

https://doi.org/10.5194/egusphere-2025-1125
Preprint. Discussion started: 25 April 2025

.459 for the second transect). For other groups, significant differences were only observed for Other_organisms between B and A for both transects and between F and B for the second transect.

Figure 8 illustrates the theoretical community distribution at the front, derived from a combination of communities from water masses A and B (Sect. 2.8.3). The positioning of theoretical front stations (*f{t}*) is displayed within the PCA_Community of Figure 6 (Fig. 8.a). For the first transect (Fig. 8.b), the α value (in Eq. 6) is low for the 0-100 m and 200-400 m layer (respectively 0.24 and 0.17) but high for the intermediate layer (0.75). This suggests that the front is influenced by processes other than just the dynamics of water masses, for instance DVM through the 100-200 m layer. For the second transect, alpha is close to 1, even equal to 1 for the deeper layers, therefore the front is very similar to water mass A (Fig. 8.c).

A notable feature is the position of *f{t}* stations compared to observed *f* stations within the reduced PCA space. Focusing on the first transect (Fig. 8.b), observed *f* stations appear displaced relative to the *f{t}* stations. Indeed, observed *f* stations are positively shifted along axes 1 and/or 2. To examine these shifts, we reconstituted the theoretical concentrations at these *f{t}* stations and then compare them to those at the *f* stations. In the 0–100 m layer, the observed shift is driven by a 103% higher concentration of Cnidaria at the front relative to the expected value at *f{t}*, while all other groups decline (average decline of 49%). In the 100–200 m layer, the discrepancy between *f* and *f{t}* is explained by a 73% higher concentration of Foraminifera at *f*, while all other groups decrease (average decline of 47%). In the 200–400 m layer, the shift is explained by a pronounced 458% higher concentration of Cnidaria and 217% higher concentration of Foraminifera at *f* compared to *f{t}*, while other groups increase by 21% on average.

In contrast, the second transect has much higher alpha values, which means a strong similarity between water mass A and F, with a strong domination of copepods in both water masses (Fig. 6). Thus, deviations between *f{t}* and *f* are very low and could not be analyzed.

3.4.3 Size and taxonomic composition of copepods

In the 0–100 m layer, copepod size structure differs most strongly, with stations *a* and *f* dominated by larger individuals (>950 µm; Fig. 9), and *b* stations by smaller ones. Meanwhile, the PCA_Size shows a much more heterogeneous distribution for the *b* stations. PCA_Size with stations M included as supplementary individuals is provided in Appendix (Fig. A5). As depth increases, size composition becomes more homogeneous, with all stations clustering near the PCA center, but slightly shifted toward highest size. Indeed, there is a decrease in Pseudo-F with depth, respectively 4.85, 1.13 and 0.98. This concentration near the PCA center and the decrease in Pseudo-F indicate a gradual decrease in variability among the deep stations, i.e., the differences between stations become less pronounced. This is also observed in the PCA_Community but it is more pronounced here for the copepod size composition.

Furthermore, to assess whether a finer taxonomic resolution of copepods could provide additional insights beyond the analysis of the whole zooplankton community (Sect. 3.4.1), we performed a PCA (Fig. A6) subdividing copepods into seven categories that accounted for more than 1% of total copepod concentration (see in Table 4). This finer taxonomic resolution confirmed the similarity between water mass A and the front, which were differentiated from water mass B, as already observed in PCA_Community.

https://doi.org/10.5194/egusphere-2025-1125
Preprint. Discussion started: 25 April 2025

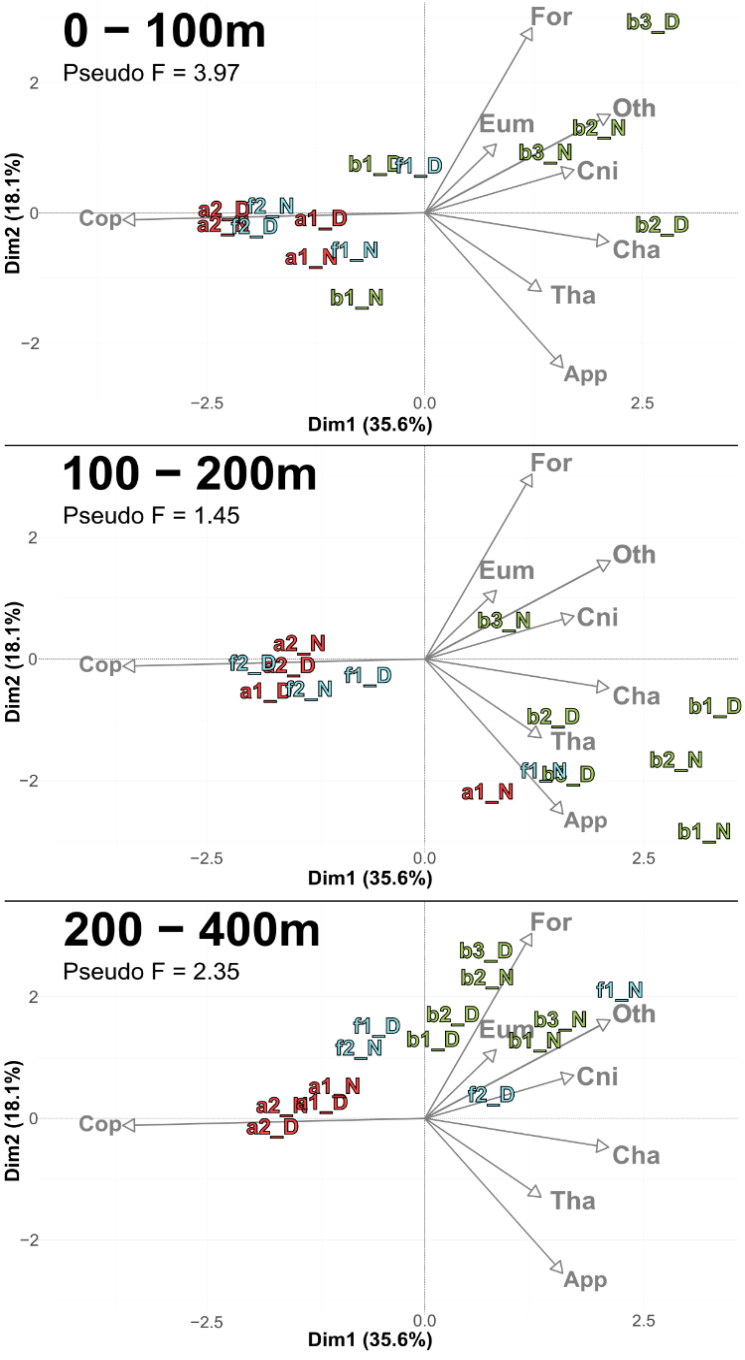

Figure 6. PCA_Community illustrating the composition of communities, based on relative concentration data (Hellinger transformation) from all stations for each reconstructed layer (a) 0-100 m, b) 100-200 m, c) 200-400m). The axis computed for 0 – 400 m were used for the three layers. Colors refers to the water mass (red for A, green for B, cyan for F). In 0-100 m: stations *a2_N* and *f2_D* overlap at dim1 = -2.3 and dim2 = -0.3. In 100-200 m: stations *a2_D* and *f2_D* overlap at dim1 = -2 and dim2 = -0.1; *f1_N* and *b1_D* overlap at dim1 = 1.9 and dim2 = -1.8. In 200-400 m: stations *a1_D* and *a2_N* overlap at dim1 = -1.8 and dim2 = 0.3.

https://doi.org/10.5194/egusphere-2025-1125
Preprint. Discussion started: 25 April 2025

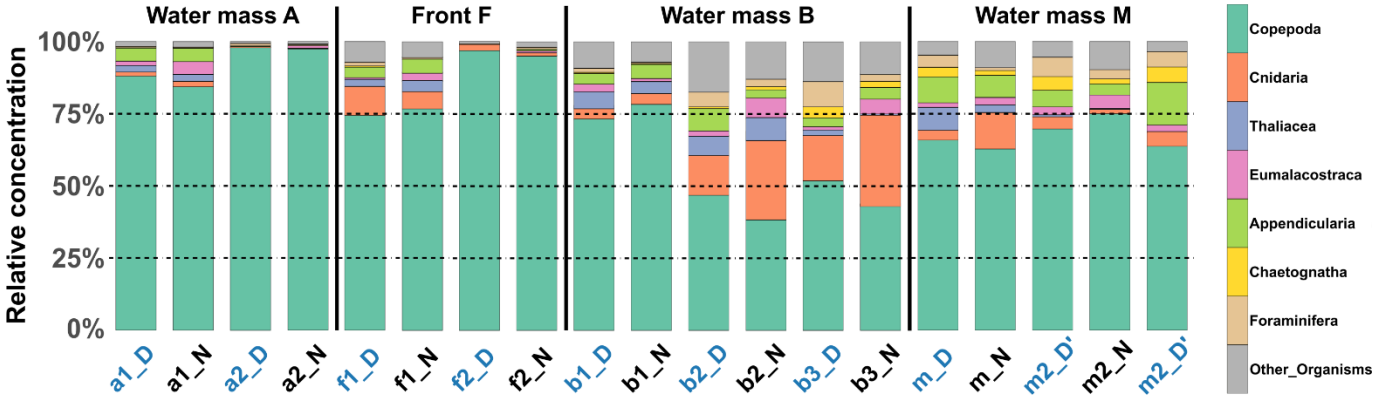

Figure 7. Relative concentration of taxonomic groups across all stations. Sorted by water mass and averaged across the three sampled layers at each station (0–100, 100–200, and 200–400 m). Colors of stations names refers to the period of the day (blue for midday and black for midnight).

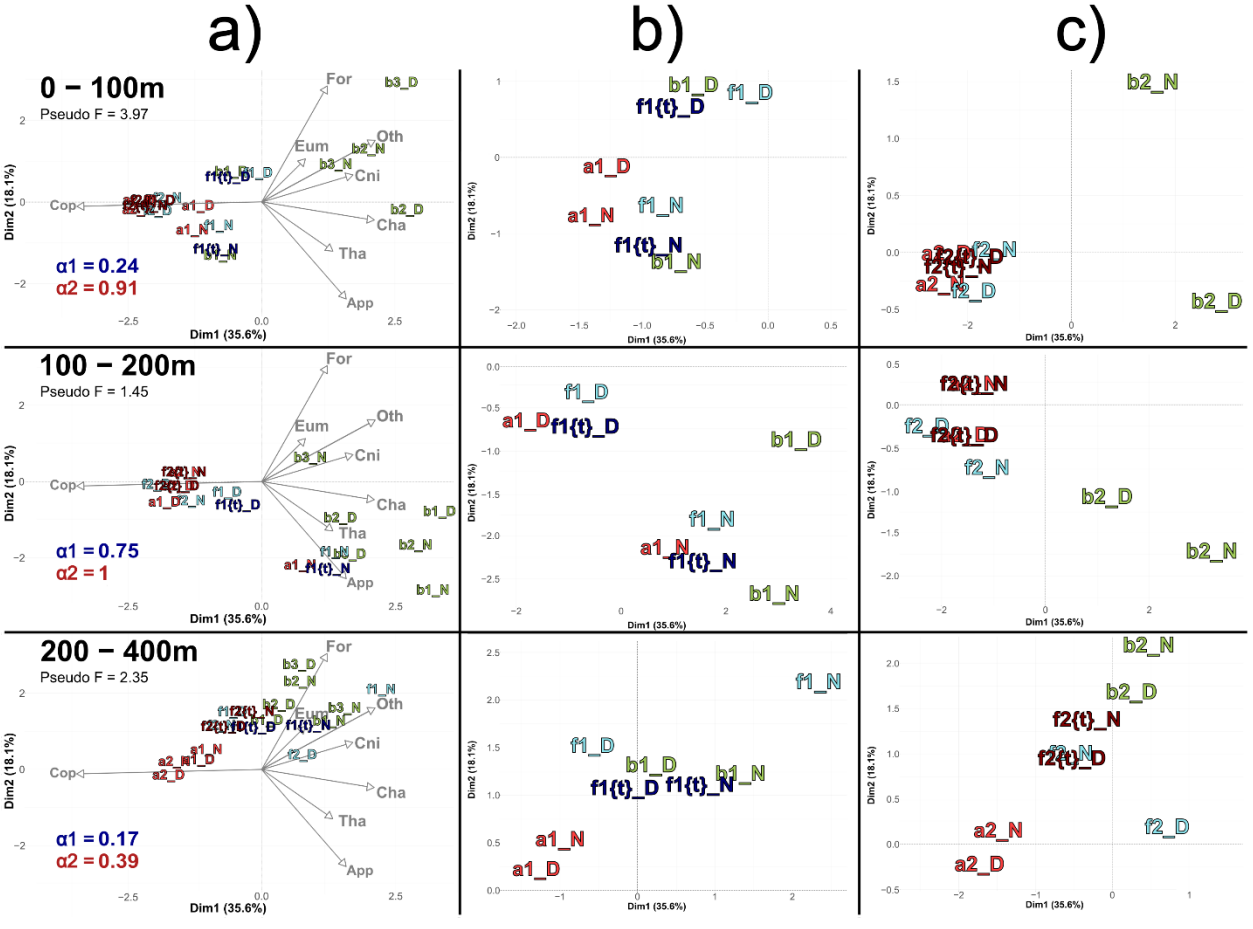

Figure 8. a) PCA_Community illustrating the composition of communities, based on relative concentration data (Hellinger transformation) from all stations for each reconstructed layer (same as figure 5). The closest theorical *f{t}* of each observed *f* is plotted, with the corresponding α_1 and α_2 values of each *f{t}*'s couple for the 1st and 2nd transect, respectively. b) Zoom for the stations of the 1st transect. c) Zoom for the stations of the 2nd transect. In c), in 0-100 m stations *a2_D, a2_N, f2_D, f2_N, f2{t}_D* and *f2{t}_N* overlap at dim1 = -2.2 and dim2 = -0.2. In 100-200 m stations *a2_D, f2_D* and *f2{t}_D* overlap at dim1 = -1.8 and dim2 = -0.3; *a2_N* and *f2{t}_N* overlap at dim1 = -1.6 and dim2 = 0.2. In 200-400 m stations *f2_N* and *f2{t}_D* overlap at dim1 = -0.4 and dim2 = 0.9.

https://doi.org/10.5194/egusphere-2025-1125
Preprint. Discussion started: 25 April 2025

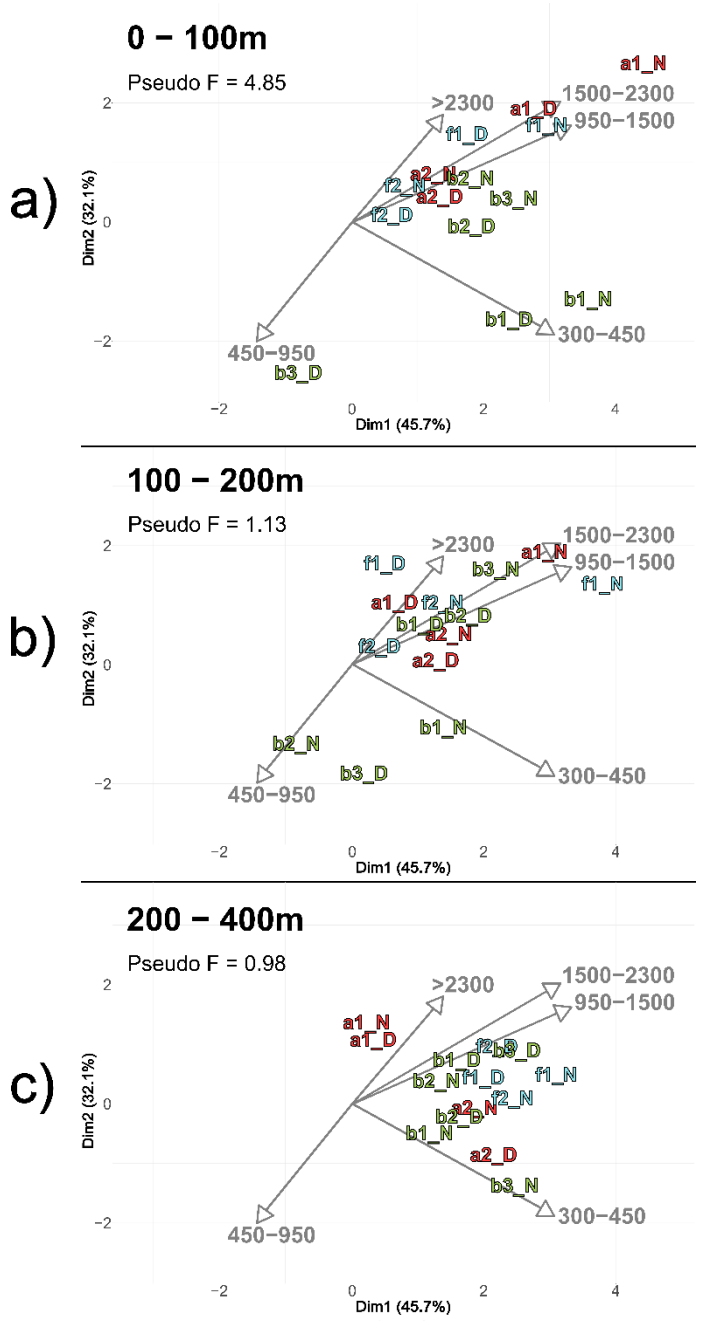

Figure 9. PCA_Size illustrating the body size composition of copepods, based on relative concentration data (Hellinger transformation) from all stations for each reconstructed layer (a) 0-100 m, b) 100-200 m, c) 200-400m). The size classes (in μm) were defined according to those from NBSS. The axis computed for 0 – 400 m were used for the three layers. Color refers to the water mass (red for A, green for B, cyan for F). In 0-100 m: stations *a2_N* and *b2_N* overlap at dim1 = 1.6 and dim2 = 0.7. In 200-400 m: stations *b3_D* and *f2_D* overlap at dim1 = 2.3 and dim2 = 0.8; *a2_N* and *b2_D* overlap at dim1 = 1.8 and dim2 = -0.2.

https://doi.org/10.5194/egusphere-2025-1125
Preprint. Discussion started: 25 April 2025

4 Discussion

4.1 Zooplankton concentrations and community structure across water masses

The spatial differences between water mass A and B in late spring can be linked to the regional hydrological and ecosystem functioning of the NWMS in the post-bloom period (D'Ortenzio and Ribera d'Alcalà (2009)). Water mass A has its origin in the Liguro-Provencal area (NWMS), characterized by intense convection and mixing (Barral et al. (2021)), high nutrient concentrations (Severin et al. (2017)) and more productivity (Mayot et al. (2017); Hunt et al. (2017)) with the formation of a deep chlorophyll maximum around 50 m (Fig. S3; Lavigne et al. (2015); Doglioli et al. (2024)). Water mass B in the southern part of the NBF comes from the epipelagic waters of the Algerian basin, which are warmer and fresher than waters from the NWMS, with virtually permanent stratification and a DCM deeper than 50 m (Fig. S3; Lavigne et al. (2015)).

In the transitional post-bloom period (April-May) encountered during the BioSWOT-Med cruise, water mass A was nutrient-richer than water mass B with mean nitrate (phosphate) concentrations in the euphotic layer ranging 0.64-1.27 (0.003-0.144) µM in A compared to 0.04-0.44 (below detection limit-0.003) µM at B. Those contrasts also appeared at 500 m depth, nitrate (phosphate) concentrations ranging 8.38-9.43 (0.34-0.40) µM in A compared to 7.49-8.89 (0.26-0.36) µM in B (Joël et al., 2025, submitted). Water mass A shows higher zooplankton stocks strongly dominated by copepods and larger forms whereas in water mass B, and community structure is dominated by small sizes and slightly more diversified within the non-copepod organisms (Fig. 4, 9), consistent with Fernández de Puelles et al. (2004).

Mesozooplankton data from the two transects across the NBF during the BioSWOT-Med campaign can only be compared with a very limited number of previous observations, particularly in the vicinity of the front. The DEWEX (2013) campaigns (Conan et al. (2018)), studied dense water formation and zooplankton dynamics during the winter-spring transition (Donoso et al. (2017)). A comparison of zooplankton concentrations and biomasses (converting our biovolumes to biomass using DW/WW of 10%, and 1 mg WW equal to 1 mm^3) between the two campaigns is presented in Table 3. The table shows, for DEWEX, low zooplankton concentrations and biomasses in the DCZ during winter. In spring, this pattern reverses with higher zooplankton stocks in the DCZ and lower in the periphery. During BioSWOT-Med, water mass A showed higher zooplankton concentrations than water mass B and F in the first transect, with the reverse pattern in the second transect (Table 3, Fig. 2). This overall decrease during BioSWOT-Med might be explained by the 10-day interval between the two transects in a phase of seasonal decline in zooplankton stocks in the convection zone (Berline et al. (2011); Auger et al. (2014)). Additionally, the storm occurring between the two transects could have influenced these decreases.

Table 3. Overview of concentrations and biomasses of zooplankton sampled during DEWEX (2013) and BioSWOT-Med campaigns. The depth range column indicates the vertical extent of the water layer considered for the calculation. DCZ stands for Deep Convection Zone. For BioSWOT-Med, values are given as the mean between day and night samples ± standard deviation

Campaign	Season	Region	Location	Concentration (ind/m^3)	Biomass (mg DW/m^3)	Depth range (m)
DEWEX 2013	Winter (February)	DCZ (A)	Near LION Station (42°04′ N, 4°38′ E)	200	5	0-250
		DCZ Periphery / Balearic (B)	North of Menorca Island	650	10	0-250
	Spring (April)	DCZ (A)	Near LION Station	4400	100	0-250
		DCZ Periphery / Balearic (B)	North of Menorca Island	2000	30	0-250
BioSWOT-Med	Late Spring (May)	Water mass A (Transect 1)	see Table 1	1848 ± 133	29 ± 4	0-200
		Water mass B (Transect 1)		881 ± 212	8 ± 3	0-200
		Front F (Transect 1)		615 ± 44	9 ± 2	0-200
		Water mass A (Transect 2)	see Table 1	745 ± 27	7 ± 2	0-200
		Water mass B (Transect 2)		333 ± 9	14 ± 3	0-200
		Front F (Transect 2)		983 ± 155	6 ± 1	0-200

https://doi.org/10.5194/egusphere-2025-1125
Preprint. Discussion started: 25 April 2025

Another interesting pattern is the highest percentage of copepods in mesozooplankton found in water mass A (around 85%) compared to water mass B (around 40%), which is consistent with other observations made in the same water masses (Nowaczyk et al. (2011); Fierro-González et al. (2023); Fernández de Puelles et al. (2023)). However, these previous observations in the NWMS were not dedicated to the NBF.

This absence of elevated zooplankton concentration and biomass at the NBF is consistent with observations from other NWMS frontal systems, such as those associated with the Northern Current in the Ligurian(Prieur and Sournia (1994); Boucher et al. (1987); Panaïotis et al. (2024)) and the Catalan seas (Alcaraz et al. (2007); Saiz et al. (2007)). In both areas, the front does not appear to be an area of higher zooplankton biomass than adjacent waters (Boucher et al. (1987); Panaïotis et al. (2024); Alcaraz et al. (2007); Saiz et al. (2007)), but it is the site of higher physiological rates (spawning rates, larval growth) of the organisms (Boucher et al. (1987); Alcaraz et al. (2007); Saiz et al. (2007)), enhanced by higher prey densities and turbulence levels (Alcaraz et al. (2007)). Studies of species distributions have shown that the front associated with the northern current can also represent a barrier for coastal species in their distribution to the central zone (Pedrotti and Fenaux (1992); Saiz et al. (2014)), or conversely, from the central zone to the coast (Berline et al. (2013)).

4.2 Complexity of concurrent processes impacting zooplankton biomass distribution at front

The decline in zooplankton concentration at the front during the first transect (Fig. 2) could reflect specific hydrological and physical mixing characteristics of the northern Balearic front (Salat (1995); Alcaraz et al. (2007)), where dynamic turbulence and horizontal dynamics appeared less favourable for biomass accumulation. Actually, while turbulence at fronts is known to enhance nutrient diffusion to phytoplankton, promoting enriched food webs for zooplankton (Kiørboe (1993); Estrada and Berdalet (1997)), it can also increase encounter rates between particles and consumers, influencing community interactions (Rothschild and Osborn (1988); Alcaraz et al. (1989); Saiz et al. (1992); Caparroy et al. (1998)). Indeed, the front in our area of interest, sampled by Lagrangian drifters at 1 and 15 m depth (Demol et al. (2023)), showed prevailing along-front deformation and patches of water mass convergence and divergence inducing variable vertical velocities up to approximately +/- 1 mm/s in the upper 15 m sea layer (Berta (2025)). Moreover, the core of the front, as identified by ADCP transects (Petrenko et al. (2024)), is found within 100 m depth and 20 km width. Consequently, considering the frontal spatial scales, as well as the divergence and the vertical transport magnitude and variability, we expect that our results do not reveal significant effects beyond 100 m depth and that mixing has shorter time scales compared to zooplankton development times (several weeks to months). In a study of 154 glider-resolved fronts across the California Current System, Powell and Ohman (2015a) found that zooplankton biomass was often, but not always, enhanced, also indicating variations in matchup of frontal duration and zooplankton development time. Finally, our campaign took place in late April to early May, corresponding to the post-bloom period (Fig. A3, A. Bosse, pers. comm.), when phytoplankton biomass levels are already too low to sustain optimal growth of specific zooplankton groups.

https://doi.org/10.5194/egusphere-2025-1125
Preprint. Discussion started: 25 April 2025

4.3 Investigating the front: mixing zone or distinct community?

A fundamental question in this study was whether the front is a mixture of communities from water masses A and B, or if it hosts a distinct community with notably different concentrations, or even the presence of new taxa. Our results indicate that the front is very similar to water mass A in several aspects: the taxonomic composition of zooplankton communities (Fig. 6), the body size distribution of copepods dominated by large individuals (Fig. 9), and the relative concentration of copepods, which decreases from A to F to B (Fig. 7). Moreover, in the 0-100 m layer, the shifts between the projections of *f* and *fT* (Fig. 7) suggests a less disruptive influence of the front on Cnidaria and Foraminifera, likely because these groups were mainly represented by small forms (e.g., ephyrae) with limited swimming ability that may benefit from the accumulation of prey at the front. In contrast, the pronounced decrease in Thaliacea, largely composed of salp chains with strong vertical migration capacity, may reflect active avoidance of physical (e.g., turbulence) and trophic (e.g., high particle load) conditions associated with the frontal region.

We note that the primary differences among taxonomic categories (Table 2) across the front concern not the most abundant groups, but secondary groups: Cnidaria, Foraminifera and Eumalacostraca for 0-100 m; Cnidaria and Foraminifera for 100-200 m. In other frontal studies, some taxa have been found more abundant than in adjacent waters (Molinero et al., 2008). Gastauer and Ohman (2024) similarly reported front-related increases in appendicularians, copepods, and rhizarians, underscoring that zooplankton community composition is shaped by species-specific responses. Biomass peaks also depend strongly on the taxa considered (Mangolte et al., 2023). However, in our analyses, we never focus on a single taxon, but rather on groups of organisms (Table 2) or on the whole sampled mesozooplankton.

To answer our initial question, the results suggest that for the first transect, the front is indeed a mix of A and B communities, but it also shows higher concentrations of organisms such as Cnidaria, Foraminifera and Chaetognatha. For the second transect, the storm of the previous days may have altered the community structure (a hypothesis that will be further discussed in Sect. 4.5), making it difficult to draw definitive conclusions.

4.4 Other potential factors affecting zooplankton structure

The method used to estimate concentrations in the 100–200 m and 200–400 m layers relied on subtracting successive hauls (Sect. 2.6). While this approach was unavoidable given the sampling design, it introduces several potential sources of error: it is sensitive to zooplankton patchiness over short time scales and may produce inconsistencies between layers. Contamination during retrieval cannot be excluded, and in some cases, subtraction yielded negative values which were set to zero. To place our data in context, we compared our relative vertical distribution to reference values reported by Di Carlo (1984), who found approximately 57% of zooplankton in 0–100 m, 27% in 100–200 m, and 16% in 200–400 m. In our dataset, mean relative concentrations were 46.2 ± 18.2% in 0–100 m, 26.9 ± 18.5% in 100–200 m, and 26.8 ± 15.5% in 200–400 m. Although Di Carlo (1984) used different net mesh size and did not separate day and night sampling, this comparison provides useful context. Therefore, concentrations in the upper 0–100 m layer are accurate. However, uncertainties remain in the reconstructed deeper layers, and results from these depths should therefore be interpreted with caution.

In addition to hydrological drivers, two processes may act as potential confounding factors when interpreting zooplankton community structure. First, DVM modifies the vertical distribution of many taxa, indeed in our samples, taxonomic and size distributions of migrant zooplankton were more similar between 0–100 m and 100–200 m layers at night, and between 100–200 m and 200–400 m layers during the day (Sect. 3.3, Fig. 4, 9). This pattern reflects the well-documented behaviour of copepods and eumalacostracans performing large-amplitude DVM, in particular species of Pleuromamma, Euchaeta, and Heterorhabdus, which may migrate within the upper 400–500 m (Andersen and Sardou, 1992; Andersen et al., 2001b; Isla et al., 2015; Guerra et al., 2019). Furthermore, the high taxonomic heterogeneity in the 100–200 m layer and the similarity between the 0–100 m and 200–400 m layers both suggest DVM, with the 100–200 m layer acting as a transitional zone.

Second, an intense wind-storm occurred between the two BioSWOT-Med transects (NW winds, peaking on 2 May). While glider data indicated only a limited deepening of the mixed layer (from ~15 m to ~30 m) and moderate changes in chlorophyll-a fluorescence (no dilution of the DCM after the storm, Fig. A3), some changes in zooplankton composition in the 0–100 m layer may reflect storm-induced mixing and dilution. Similar short-term effects of storms have previously been reported in the NW Mediterranean, including increased nauplii production linked to adult spawning but reduced copepod biomass, and upward aggregation of nauplii and small-sized copepods in the upper 40 m (Andersen et al., 2001a,b; Barrillon et al., 2023). In our case, the comparison of concentration between the two transects revealed significant differences for the 0–100 m layer, but not in deeper layer, therefore potentially linked to the storm (Table 3). In this surface layer, small and mid-sized copepods, chaetognaths, and cnidarians were the most affected, whereas large migrant copepods, such as *Pleuromamma* and *Euchaeta*, appeared weakly impacted. A similar trend was observed for Calanoida, which includes both small and large, migrant and non-migrant species. Analyses of the whole

https://doi.org/10.5194/egusphere-2025-1125
Preprint. Discussion started: 25 April 2025

planktonic community response to the storm (including phytoplankton) are required to better understand the observed zooplankton changes.

However, because the two transects were 9 days apart and approximately distant of 50 km, the present dataset does not allow storm effects to be unambiguously disentangled from general temporal or spatial variability. The storm should therefore be considered as one, but not exclusive, driver of the observed changes.

The observed variability in zooplankton concentrations over time and space underscores the complexity of concurrent processes acting at different scales, such as DVM or storm events that interact with the hydrological processes creating the front.

Table 4. Results of ANOVA tests (H0: no differences of averages between the first and the second transect) performed on the eight taxonomic groups and seven copepod subgroups (subgroups with total concentration greater than 1% of the overall copepod assemblage). For each significant ANOVA result ($p < 0.05$), a Tukey's Honest Significant Difference test was applied to identify differences between the first and the second transect for each water mass (shown in the last four columns). For layers 100-200 m and 200-400 m, no significant differences were found.

Type of analysis	Depth	Taxonomic group / species	ANOVA p-value	p-value A1st vs A2nd	p-value B1st vs B2nd	p-value F1st vs F2nd	p-value M1st vs M2nd
ANOVA Depth	0-100 m	Appendicularians	0.124				
		Chaetognatha	**0.039** *	**<0.001** ***	0.0659	**<0.001** ***	0.108
		Cnidaria	**<0.001** ***	**<0.001** ***	**<0.001** ***	0.418	0.765
		Copepoda	**<0.001** ***	0.189	**<0.001** ***	**<0.001** ***	0.617
		Eumalacostraca	0.534				
		Foraminifera	0.429				
		Other_organisms	0.375				
		Thaliacea	0.929				
ANOVA Copepod species	0-100 m	Calanoida	0.255				
		Centropages spp.	**0.014** *	**0.002** **	0.104	**< 0.001** ***	1
		Corycaeidae spp.	**0.0104** *	**< 0.001** ***	0.797	**< 0.001** ***	0.992
		Euchaeta	0.581				
		Oithona	**0.0231** *	0.448	**0.0197** *	0.923	0.876
		Oncaeidae	**0.015** *	**< 0.001** ***	**0.031***	**0.025** *	0.87
		Pleuromamma spp.	0.928				

https://doi.org/10.5194/egusphere-2025-1125
Preprint. Discussion started: 25 April 2025

5. Conclusion

To our knowledge, this study represents the first detailed investigation of the fine-scale zooplankton distribution of the North Balearic Front in late spring, linking finescale dynamics to mesozooplankton distributions. Our findings reveal that the North Balearic Front exhibits characteristics more akin to a boundary between water masses than a zone of pronounced biological accumulation.

Key observations include the stratified vertical distribution of zooplankton communities, with distinct taxonomic compositions in the surface, intermediate, and deeper layers, and a progressive homogenization of community structure with depth. DVM was particularly evident, underscoring the dynamic nature of zooplankton behaviour in relation to environmental gradients. Moreover, post-storm analyses highlighted the susceptibility of these communities to episodic weather events, which can disrupt established ecological patterns.

These results challenge generalized assumptions about the ecological role of oceanic fronts. They underscore the importance of high-resolution observations across horizontal and vertical spatial scales, consideration of short temporal processes, and precise taxonomic identification to fully understand the complexity of mesozooplanktonic communities in frontal zones.

Further trophic studies based on stable isotope ratios and the biochemical composition of zooplankton and phytoplankton size classes are still needed. Such studies would help to decipher trophic interactions in the frontal area, where nutrient input is driven by physical processes. In addition, our net sampling approaches need to be complemented by continuous measurement techniques, such as autonomous gliders, bioacoustics and satellite data, with in-situ sampling to better capture the spatial and temporal variability of these systems. This approach would enable a more comprehensive assessment of how physical and biological processes interact to shape zooplankton communities at oceanic fronts.

Data Availability Statement

The Sentinel-3 data used in this manuscript are available and freely accessible to the public (https://www.copernicus.eu/en), accessed on 11 November 2024.

Author Contribution

MD was responsible for data curation, formal analysis, visualization, and conceptualization. FC and LB contributed to conceptualization and were responsible for supervision and validation. LG performed the ZooScan processing and taxonomic identification of the samples. MD prepared the manuscript with review and editing of all co-authors.

Acknowledgments

The authors thank the TOSCA program of the CNES (French Spatial Agency) which funds the BIOSWOT-AdAC project and the ANR – FRANCE (French National Research Agency) for its financial support to the BIOSWOT ANR-23-CE01-0027 project.
The FOF (French Oceanographic Fleet) and, in particular, the captain Gilles Ferrand and the crew of the R/V L'Atalante are acknowledged for their precious support during the BioSWOT-Med cruise.
M.D. Ohman and S. Gastauer were supported by U.S. National Science Foundation grant OCE-2243190.

Alice Della Penna was supported by the University of Auckland via the Faculty Research Development Fund (Grant 3724591)
Dr. Maristella Berta contribution was supported by the ITINERIS Project (IR0000032-Italian Integrated Environmental Research Infrastructures System-CUP B53C22002150006) and by CNR-ISMAR (Lerici, Italy) dedicated fundings.

https://doi.org/10.5194/egusphere-2025-1125
Preprint. Discussion started: 25 April 2025

Appendix

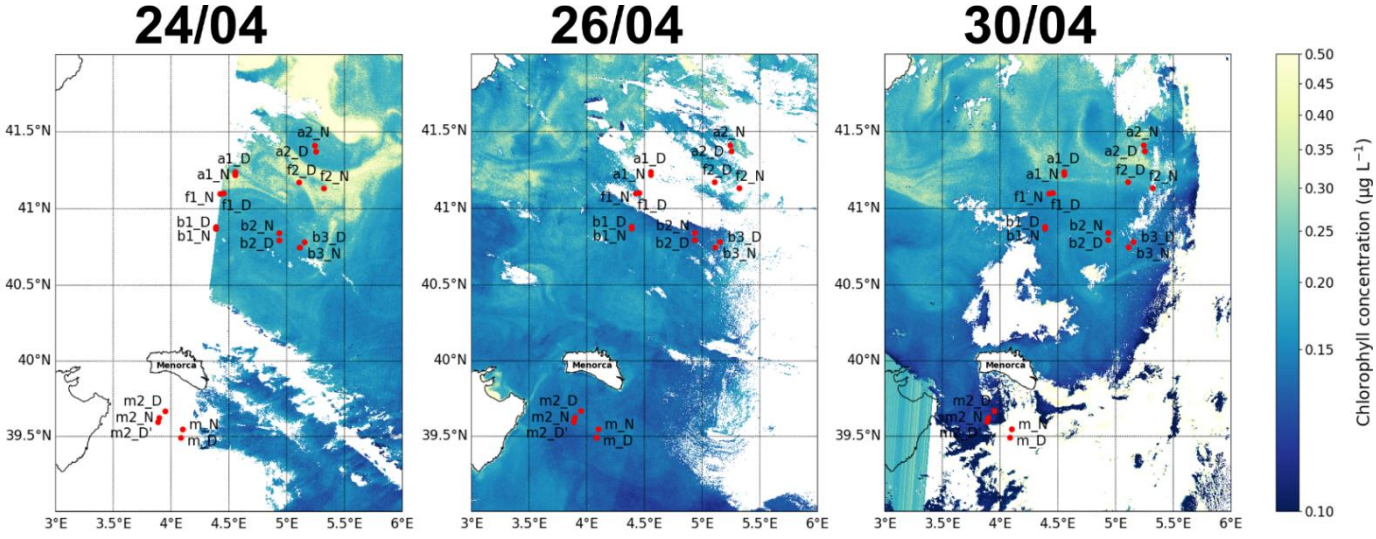

Figure A1. Maps of the sampling stations with surface chlorophyll concentration for 3 different days (as complement of Figure 1)

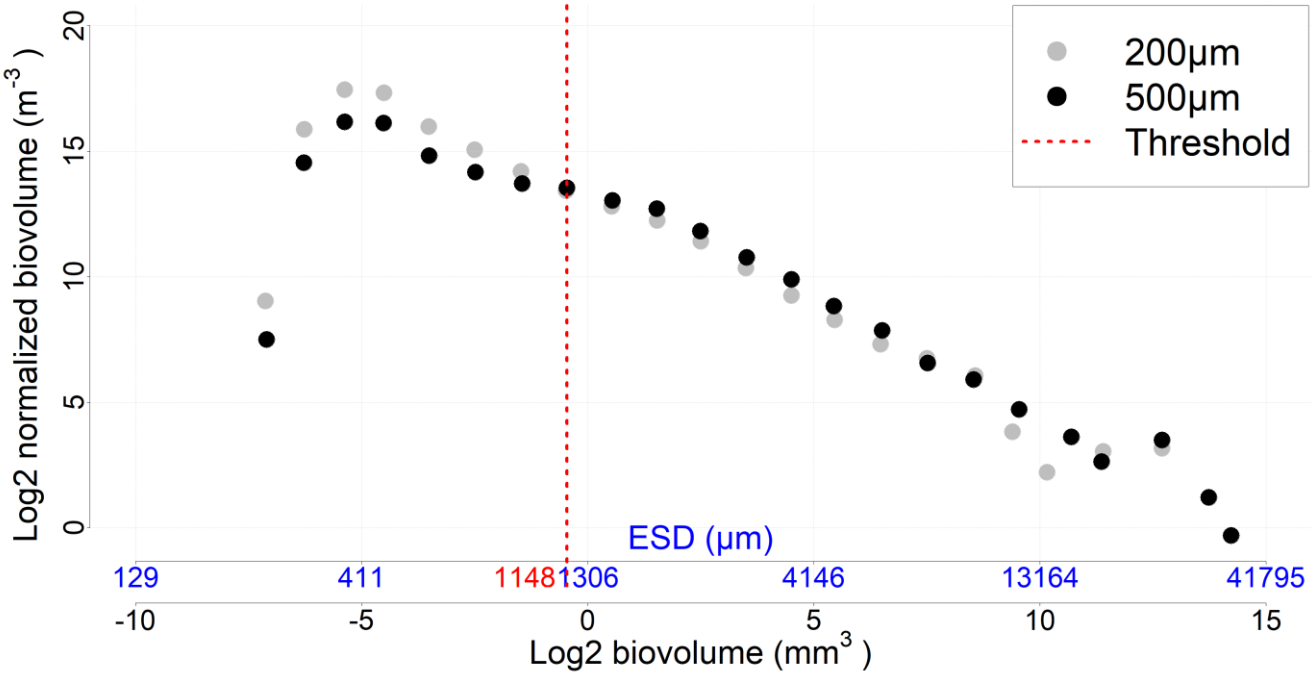

Figure A2. NBSS incorporating all data (all stations and depths) for each mesh size. The threshold value represents the organism size above which the 500 µm nets sample more efficiently than the 200 µm nets

https://doi.org/10.5194/egusphere-2025-1125
Preprint. Discussion started: 25 April 2025

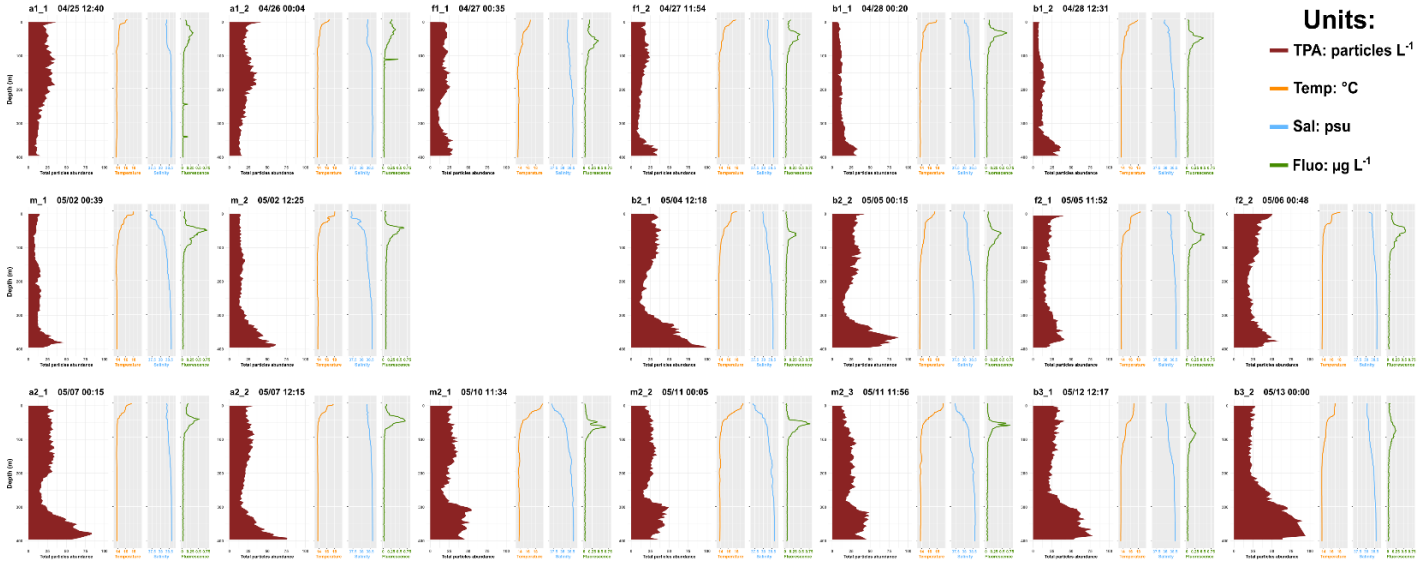

Figure A3. Total particles abundance, temperature, salinity, and fluorescence profiles

https://doi.org/10.5194/egusphere-2025-1125
Preprint. Discussion started: 25 April 2025

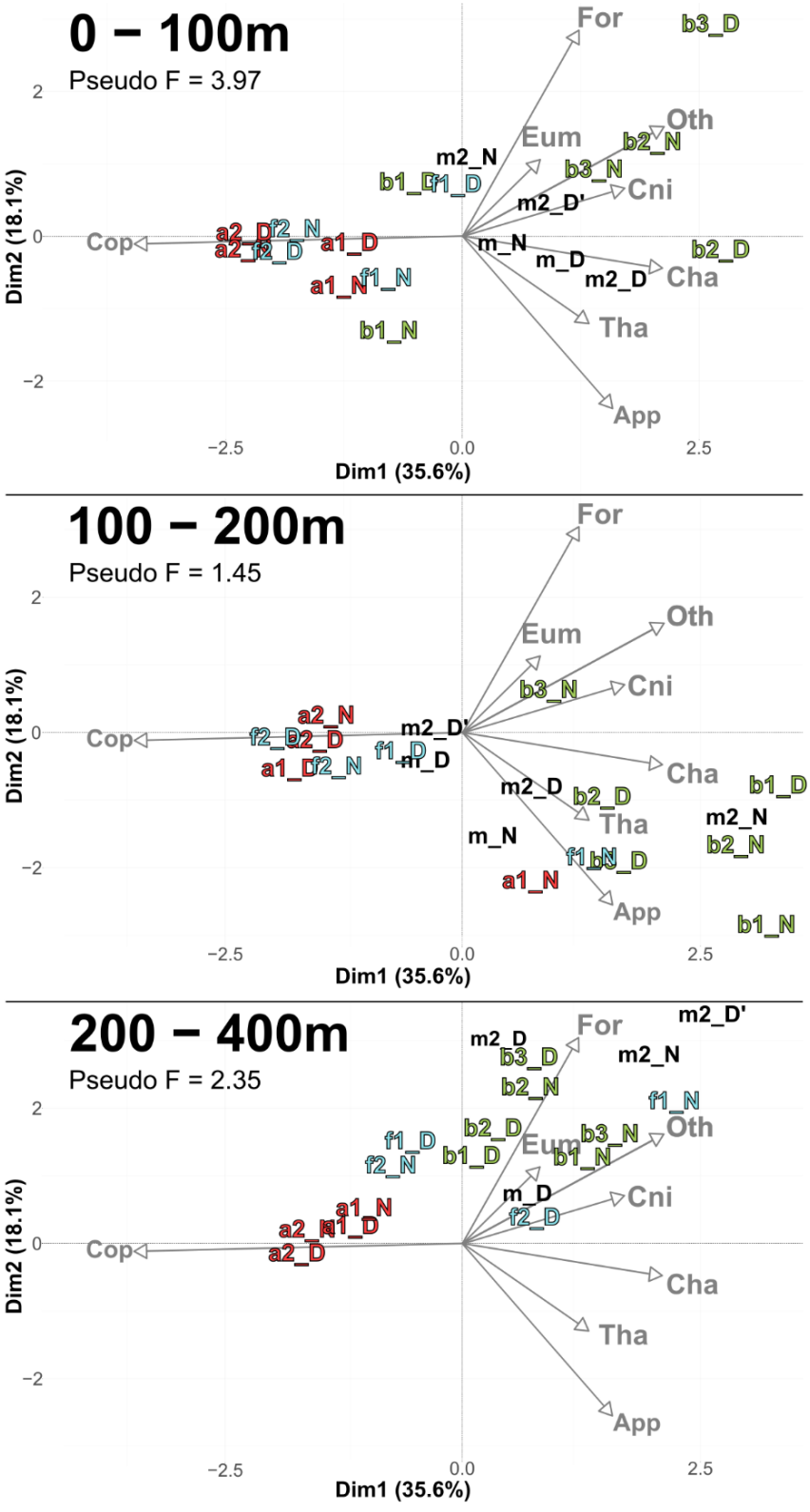

Figure A4. PCA_Community (same as Fig. 6) with M stations projected as supplementary individuals

https://doi.org/10.5194/egusphere-2025-1125
Preprint. Discussion started: 25 April 2025

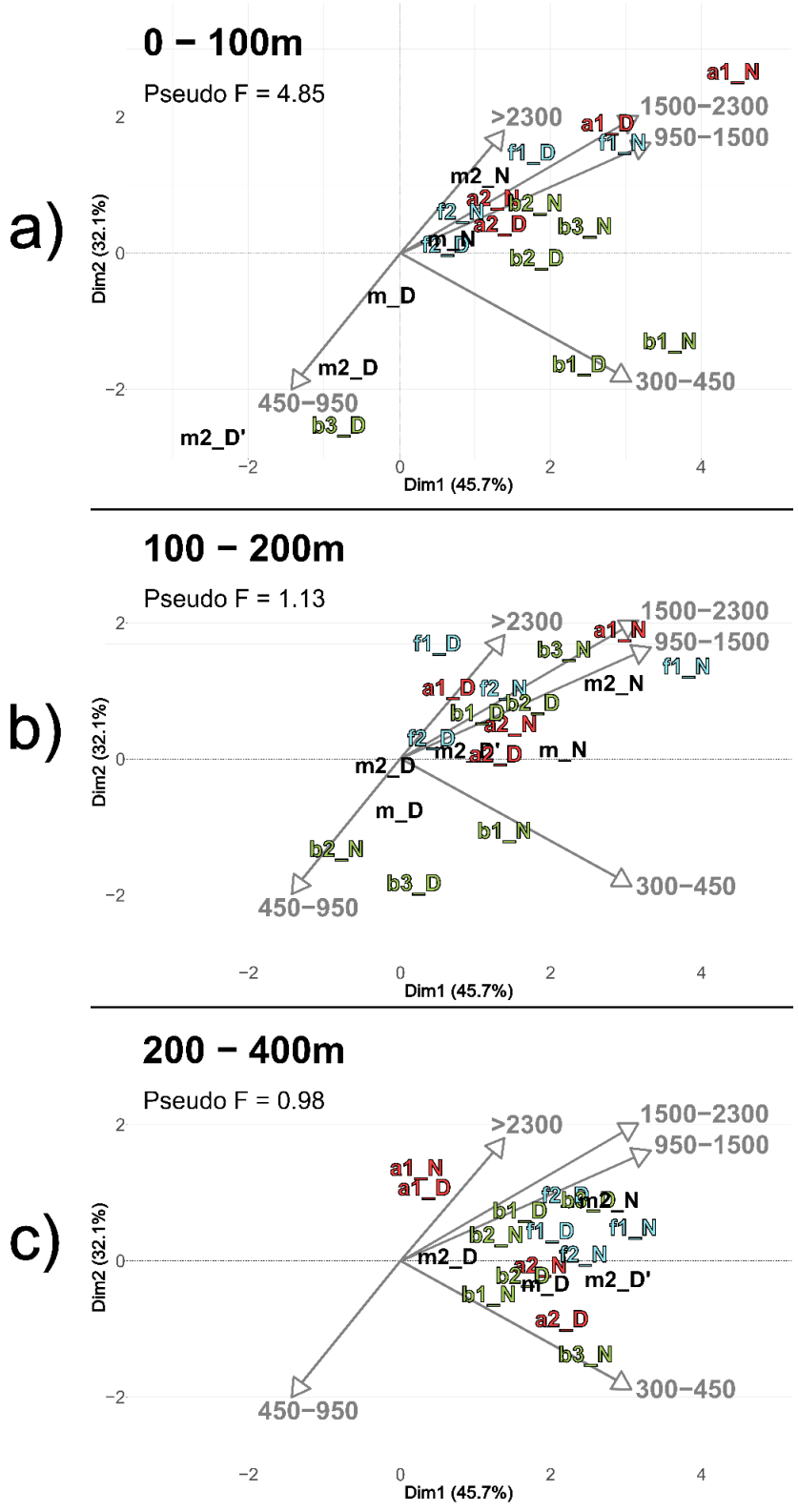

Figure A5. PCA_Size (same as Fig. 9) with M stations projected as supplementary individuals

https://doi.org/10.5194/egusphere-2025-1125
Preprint. Discussion started: 25 April 2025

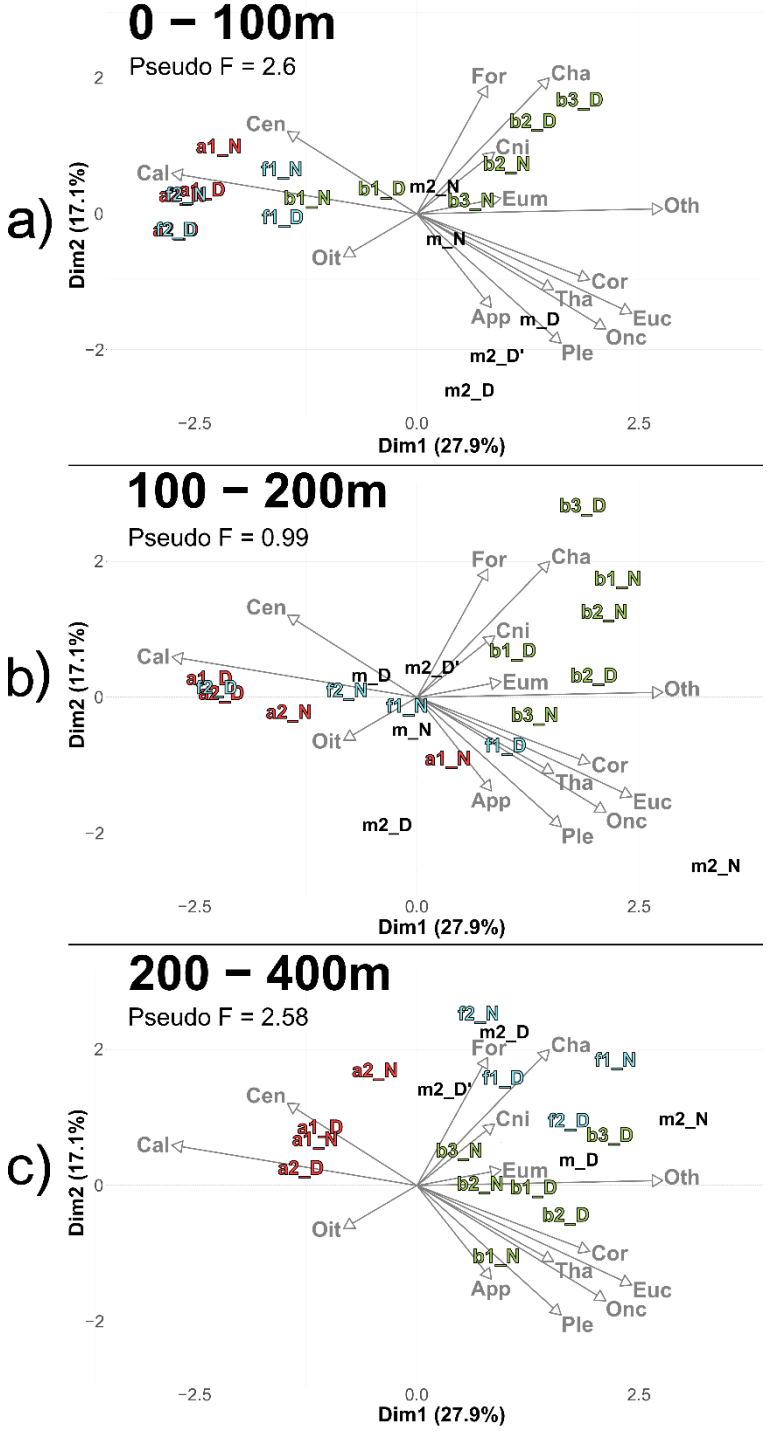

Figure A6. PCA illustrating the taxonomic composition of communities with copepods divided in seven copepod subgroups (subgroups with total concentration greater than 1% of the overall copepod assemblage). Based on relative concentration data (Hellinger transformation) from all stations for each reconstructed layer (a) 0-100 m, b) 100-200 m, c) 200-400m). The axis computed for 0 – 400 m were used for the three layers. Colors refers to the water mass (red for A, green for B, cyan for F).

https://doi.org/10.5194/egusphere-2025-1125
Preprint. Discussion started: 25 April 2025